Bolko von Roedern, MS 3212
National Center for Photovoltaics
National Renewable Energy Laboratory
1617 Cole Boulevard
Golden, CO 80401

08/15/2007

Dear Bolko,

This is the annual report of our second year in the Thin Film Partnership Program (Subcontract No. XXL-5-44205-12 to University of Nevada, Las Vegas: Characterization of the electronic and chemical structure at thin film solar cell interfaces). A brief summary and details of our activities are given below. This report is in fulfillment of the deliverable schedule of the subcontract statement of work (SOW).

Summary

This project is devoted to deriving the electronic structure of interfaces in $Cu(In,Ga)(S,Se)_2$ and CdTe thin film solar cells. By using a unique combination of spectroscopic methods (photoelectron spectroscopy, inverse photoemission, and X-ray absorption and emission) a comprehensive picture of the electronic (i.e., band alignment in the valence and conduction band) as well as chemical structure can be painted. The work focuses on (a) deriving the bench mark picture for world-record cells, (b) analyze state-of-the-art cells from industrial processes, and (c) aid in the troubleshooting of cells with substandard performance.

In the last year, we could draw a complete picture of the chemical and electronic properties of the deeply buried chalcopyrite/back contact interface. For these experiments $Cu(In,Ga)Se_2$ ("CIGSe") and $Cu(In,Ga)(S,Se)_2$ ("CIGSSe")/back contact samples prepared by the group of W. Shafarman (Institute of Energy Conversion, University of Delaware) were used. We have found a pronounced chemical interaction between absorber and back contact, namely the formation of $MoSe_2$ (and $Mo(S,Se)_2$) and a "diffusion" of Ga into the Mo layer. In addition, we could derive a tentatively flat valence band alignment at this interface.

In addition, we have investigated the CdS/CIGSe interface of samples provided by the National Renewable Energy Laboratory (M. Contreras, R. Noufi), which currently holds the world record for respective solar cell devices in terms of photovoltaic performance. Our results show that, in contrast to earlier measurements on samples from a different source, no pronounced S/Se intermixing at this interface can be observed.

Detailed Description of the Activities:

1. The deeply buried chalcopyrite/Mo interface

In the past year, we have focused on the characterization of the deeply buried interface between absorber and Mo back contact in chalcopyrite thin film solar cells. These investigations were based on two different types of samples, namely CIGSe/Mo/glass and CIGSSe/Mo/glass. Both sample types were provided by the group of W. Shafarman (IEC, U Delaware). In order to make the interface between absorber and Mo accessible for characterization by photoelectron spectroscopy (PES), we had to develop a suitable lift-off (cleavage) technique, which allowed us to cleave the absorber/Mo/glass samples at the desired interface. It was found that gluing the front side of the absorber/Mo/glass thin film stack to a stainless steel plate using a conductive (Ag-containing) ultra-high vacuum (UHV) compatible epoxy allows a subsequent division of the stack in two parts and provides the necessary conductivity for the PES measurements. Note that the "lift-off" process itself took place in a N_2-filled glovebox or glovebag, which was directly connected to the load lock chamber of the UHV surface analysis system in order to minimize contamination of the freshly prepared cleavage planes. The scheme in Fig. 1 visualizes the different investigated surfaces for each lift-off process:

(a) Surface
(b) Back Surface
(c) Mo-Side

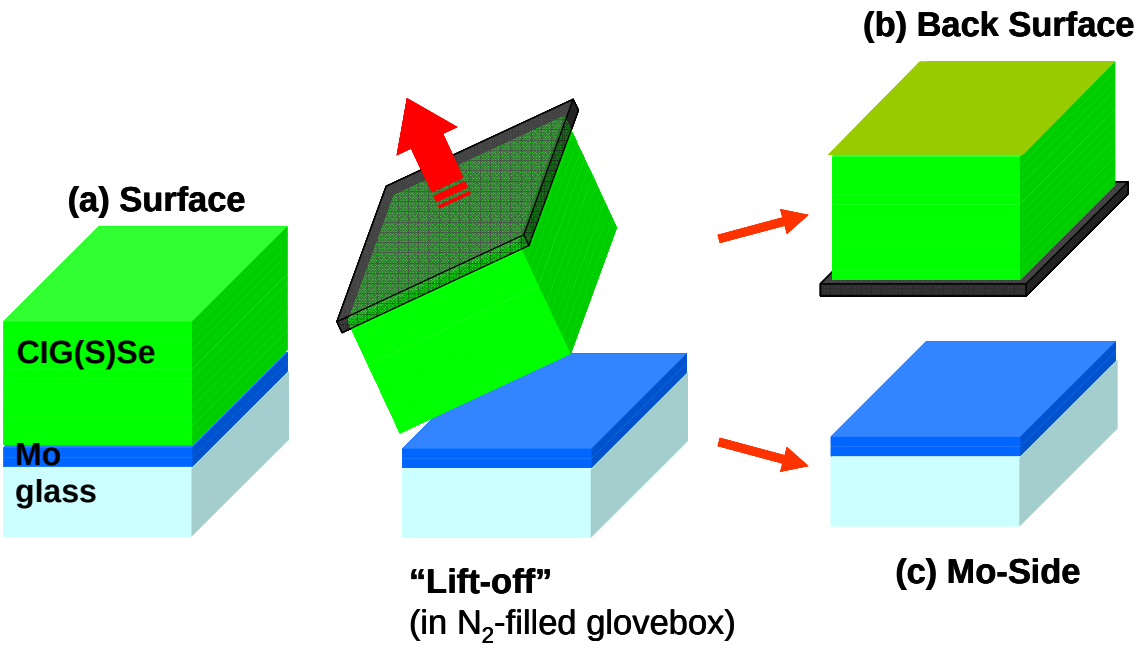

Fig. 1: Scheme of the lift-off process and visualization of the different prepared and investigated surfaces.

First, we will focus on the results gained from the investigation of the samples by X-ray photoelectron spectroscopy (XPS). Fig. 2 shows the XPS survey spectra of the Surface, Back Surface, and Mo-Side of the CIGSSe (top panel) and CIGSe (bottom panel) samples. Although the samples were handled and shipped under inert gas atmosphere and stored in ultra-high vacuum (UHV), one can observe distinct peaks which can be ascribed to C and O on the Surface (a), stemming from a contamination layer formed on the ab-

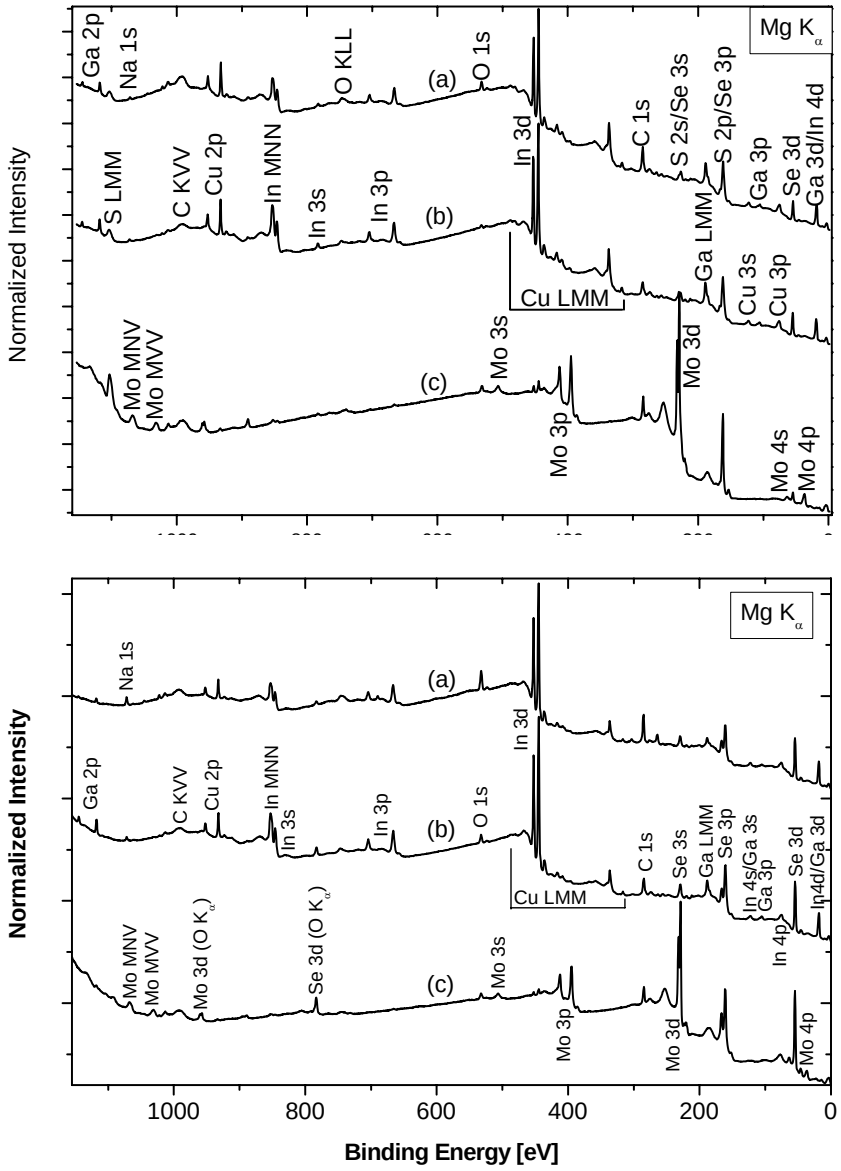

Fig. 2: XPS survey spectra of the different accessible "surfaces" before and after lifting-off the chalcopyrite absorber from the Mo/glass substrate (top: CIGSSe, bottom: CIGSe): (a) Surface, (b) Back Surface, and (c)Mo-side.

sorber surface. In contrast, we find only minor amounts of oxygen on the Back Surface (b). This shows that the applied cleavage process in an N_2 filled glovebag/glovebox and the immediate transfer of the cleaved samples into the attached UHV characterization system provides surfaces with minimized contamination (oxidation), which is of large importance for a subsequent determination of the electronic surface (and interface) structure. Note that the residual C 1s signal observed on the Back Surface points to a carbon incorporation into the absorber layer.

The intensity difference of all absorber features (e.g., Ga 2p, Cu 2p, and In 3d) between Surface and Back Surface can be explained by the different attenuation of the differently thick contamination layers. At first sight (see also discussion below) no Mo emission can be found on the Back Surface and only minor amounts of the absorber components (as indicated by the small In 3d peak - the most prominent absorber feature) can be observed on the Mo-Side. This confirms that the cleavage occurs at the absorber/Mo interface with only some chalcopyrite grains remaining on the back contact (this characteristic of the lift-off mechanism was already described in our Ref. [1]). In consequence, the comparatively large intensities of the photoemission and Auger lines of S and Se observed on the Mo Front point to the formation of a $Mo(S,Se)_2$ and $MoSe_2$ layer at the back contact for the CIGSSe and CIGSe sample, respectively. This was similarly reported/suggested in the past [1-7]. However, as shown in Fig. 3 (which shows the S 2p/Se 3p lines of the different CIGSSe-based samples), the S/Se ratio in the $Mo(S,Se)_2$

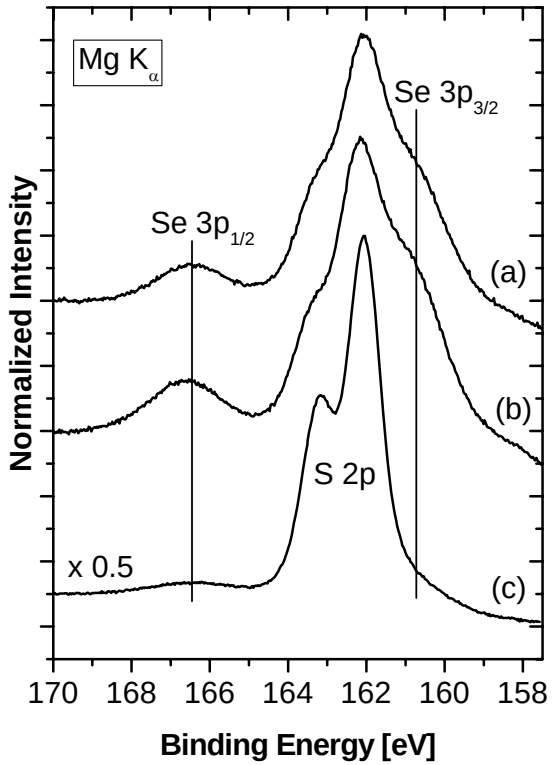

Fig. 3: S 2p/ Se 3p photoemission of the different "surfaces" before and after lifting-off the CIGSSe absorber from the Mo/glass substrate: (a) Surface, (b) Back Surface, and (c)Mo-side.

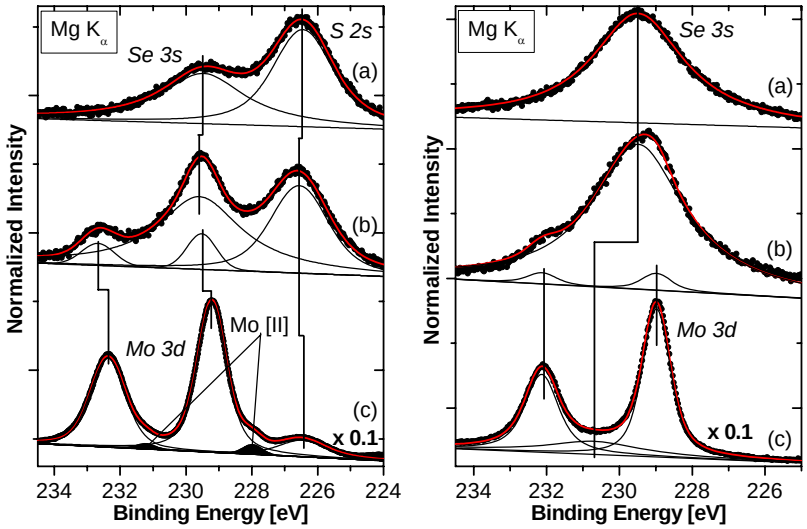

Fig. 4: (Overlapping) S 2s/Se 3s and Mo 3d photoemission lines of the different "surfaces" before and after removing the chalcopyrite absorbers from the Mo/glass substrate (left: CIGSSe, right: CIGSe): (a) Surface, (b) Back Surface, and (c)Mo-side.

film does not mirror the S/Se ratio of the absorber. In this case, the formation of MoS_2 is clearly preferred over the formation of $MoSe_2$.

A more detailed analysis of our data indicates that (besides the formation of the $Mo(S,Se)_2$) additional chemical interactions at the absorber/back contact interface take place. A detailed comparison of the S 2s/Se 3s and Mo 3d energy range for the different samples (Surface, Back Surface, Mo-Side, Fig. 4) reveals that a (minor) Mo signal at the Back Surface can be identified at both absorber/back contact structures. This agrees with our earlier X-ray emission (XES) measurements [2] of different chalcopyrite/back contact structures, which also showed Mo at the absorber back side. It is at present unknown whether this is due to Mo diffusion into the Back Surface or the presence of some residual $Mo(S,Se)_2$ from the cleavage process.

A further important result from the spectra in Fig. 4 is the finding that the $Mo(S,Se)_2$ layer (in the CIGSSe case) is apparently thinner than the $MoSe_2$ layer (in the CIGSe case), as evidenced by the residual metallic Mo 3d doublet (filled black peaks in Fig. 4, bottom left) in the CIGSSe case.

Our previous XES data also showed an accumulation/diffusion of Ga at/into the back contact [2]. Comparing the intensity of the most prominent photoemission lines of the absorber constituents (Ga $2p_{3/2}$, Cu $2p_{3/2}$, and In $3d_{3/2}$) of the Back Surface and the absorber remainders at the Mo-Side, our present XPS data confirms the accumulation of Ga. As shown in Fig. 5, we find that the Ga 2p intensity from the Mo-side is significantly larger than the intensity of the other absorber elements; note that the peaks in Fig. 5 were normalized to the absolute intensity of the respective peaks observed for the Back Surface, and hence a larger Ga peak directly indicates the presence of additional Ga on/in the Mo-side surface.

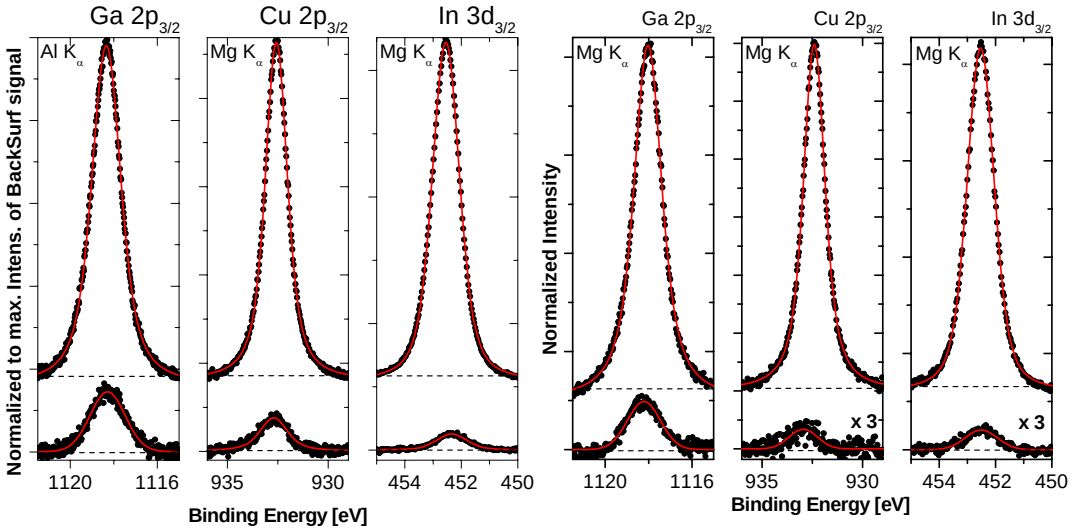

Fig. 5: Comparison of the Ga $2p_{3/2}$, Cu $2p_{3/2}$, and In $3d_{3/2}$ photoemission lines of the Back Surface (top) and absorber remainders at the Mo-Side (bottom). The intensities are normalized to the respective maximum of the Back Surface. The corresponding spectra of the CIGSSe/CIGSe samples are shown in the left and right three panels, respectively.

In the following we will focus on the comparison of the CIGSSe Surface and CIGSSe Back Surface in terms of their composition. In order to determine the

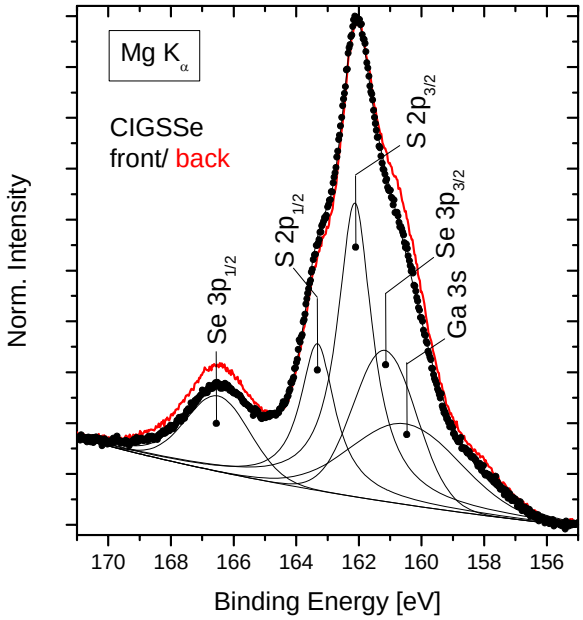

Fig. 6: Region of the S 2p, Se3p, and Ga 3s photoemission lines of the CIGSSe Surface (black dots) and CIGSSe Back Surface (red line). For the CIGSSe Surface spectrum also the corresponding fits (black lines) are shown.

Ga/(Ga+In) = X and the S/(S=Se) = Y composition of the front and back side of the $Cu(In_{1-X}Ga_X)(S_YSe_{1-Y})_2$ absorber, the S 2p/Se 3p (Fig. 6) and the Ga 3d/In 4d detail spectra (Fig. 7) are evaluated. For direct comparison of CIGSSe Surface and CIGSSe Back Surface, the spectra are normalized to their maximum. In addition, the spectra of the latter have been shifted to lower binding energies by 0.1 eV for maximal overlap. The observed higher binding energies for both, the S 2p/Se3p and the Ga 3d/In4d spectra for the CIGSSe Back Surface point to an increased surface band bending compared to the CIGSSe Surface. Fig. 6 shows the region of the S 2p, Se 3p, and Ga 3s photoemission lines of the cleaved samples CIGSSe Surface (black dots) and CIGSSe Back Surface (red line). For the CIGSSe Surface spectrum also the corresponding fits (black lines) are shown. The comparison of the spectra clearly shows that the S/(S+Se) ratio at the CIGSSe Surface is higher than that of the CIGSSe Back Surface. For quantification of the S/(S+Se) ratio we have used the intensity of the S $2p_{3/2}$ and the Se $3p_{3/2}$ photoemission lines, which were determined by fitting the corresponding contributions of the spectra with Voigt area functions (exemplarily shown in Fig. 6). Due to the similar binding energies for the S 2p and the Se 3p peaks, it was legitimately assumed that the inelastic mean free paths and the analyzer characteristics are the same for the corresponding photoelectrons. Thus, for the calculation of the S/(S+Se) ratio the corresponding peak intensities were only corrected by the respective cross-sections (from Ref. [8]). In consequence, Y (the S/(S+Se) ratio) of the CIGSSe Surface and CIGSSe Back Surface was determined as 0.79 and 0.65, respectively, as shown in Table II. For the determination of X (the Ga/(Ga+In) ratio) of the CIGSSe Surface and CIGSSe Back Surface, we again have used adjacent photoemission lines (as shown in Fig. 7). The direct comparison of the Ga 3d/In 4d spectra of the cleaved samples CIGSSe Surface (black line) and CIGSSe Back Surface (red dots) reveals that X of both sample surfaces is quite similar. Indeed, the quantification of the Ga $3d_{5/2}$ and the In $4d_{5/2}$ photoemission lines determines X values (0.36 and 0.33, see Table I) which are, within the error margins, identical for the CIGSSe Surface and CIGSSe Back Surface.

Table I

sample	X Ga/(Ga+In)	Y S/(S+Se)	E_g [eV]
CIGSSe Surface	0.36	0.79	1.68
CIGSSe Back Surface	0.33	0.65	1.58

Assuming a stoichiometric absorber composition (in particular no Cu deficiency towards the absorber surface) the X and Y compositions should allow a direct (“theoretical”) estimate of the absorber band gap (E_g). Using equation (1) (Ref. [9]) we have determined E_g for the CIGSSe Surface to 1.68 eV and for the CIGSSe Back Surface to 1.58 eV (see Table I).

$$E_g = 1 + 0.13X^2 + 0.08X^2Y + 0.13XY + 0.55X + 0.54Y \qquad (1)$$

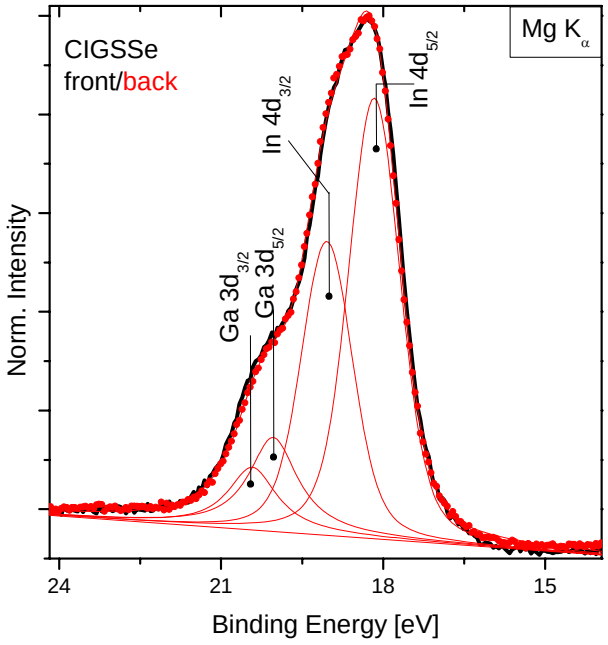

Fig. 7: Ga 3d and In 4d spectra of the cleaved samples CIGSSe Surface (black line) and CIGSSe Back Surface (red dots). For the CIGSSe Back Surface spectrum also the corresponding fits (red lines) are shown.

In order to directly *measure* the band gap at the CIGSSe Surface and CIGSSe Back Surface, we additionally characterized a set of cleaved samples with UV photoelectron spectroscopy (UPS) and inverse photoemission (IPES). The corresponding UPS and IPES spectra for the CIGSSe Surface and Back Surface are shown in Fig. 8 left and right, respectively. The linear extrapolation of the leading edge of the UPS and IPES spectra results in the position of the valence band maximum (VBM) and conduction band minimum (CBM), respectively. Thus, the sum of the absolute values of VBM and CBM reveals the electronic surface band gap E_g^{Surf}. In addition to the UPS/IPES spectra and the respective VBM, CBM, and E_g^{Surf} values of the as-prepared CIGSSe Surface (left) and CIGSSe Back Surface (right) samples, Fig. 8 also shows the electronic properties after several cleaning cycles with a mild Ar^+ beam (E_{ion} = 50 eV, $I_{sample} < 1\mu A$). As can be observed in Fig. 8, the VBM, CBM, and E_g^{Surf} values remain constant after 30 min (CIGSSe Back Surface) and 60 min (CIGSSe Surface) of Ar^+ treatment. The difference in required treatment time is most likely due to the more pronounced contamination layer on the CIGSSe Surface, as discussed above. The respective XPS survey spectra after Ar^+ treatment (not shown) also indicate clean sample surfaces without C- or O-containing contaminants. The experimentally determined electronic surface band gaps of (1.94 ± 0.15) eV for the CIGSSe Surface and (2.09 ± 0.15) eV for the CIGSSe Back Surface are larger than the band gaps calculated from the surface stoichiometry determined by XPS (see Table I). Enlarged electronic surface band gaps have in the past [10-12] been explained by the formation of a Cu-poor "Ordered Vacancy Compound" [13] or "Ordered Defect Compound" [14] surface phase, which deviates from the Cu : In+Ga : S+Se ratio of 1 : 1 : 2 forming on top of the chalcopyrite absorber. Our XPS results indeed show a Cu-poor surface stoichiometry for both, the CIGSSe Surface as well as the CIGSSe Back Surface.

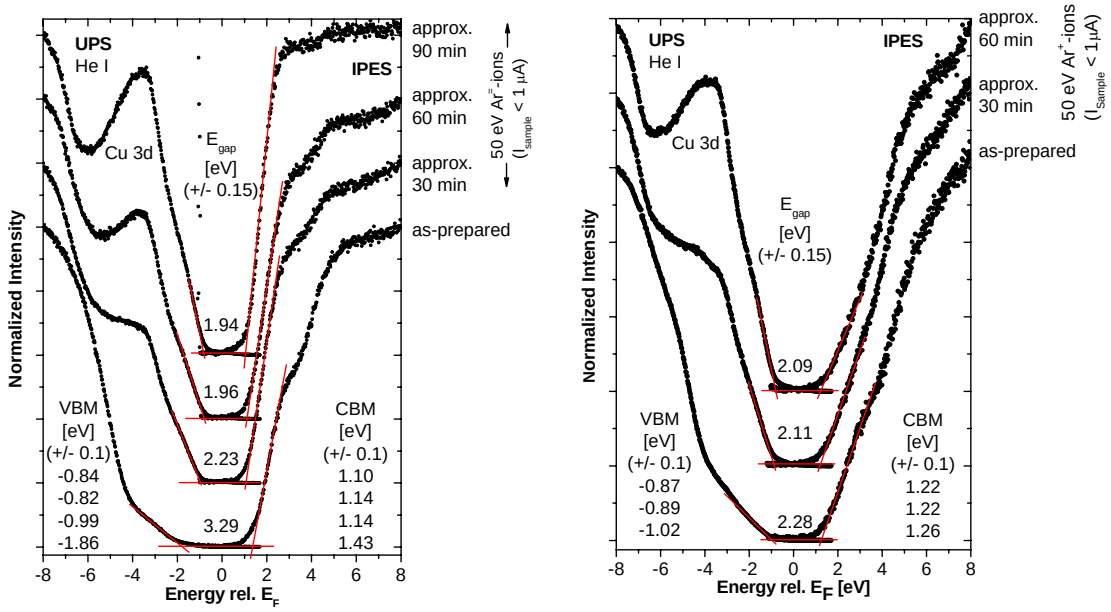

Fig. 8: UPS and IPES spectra (black dots) and derived VBM, CBM, and surface band gap values of as-prepared CIGSSe Surface (left) and CIGSSe Back Surface (right) samples. In addition, the corresponding spectra are also shown after different cleaning steps by a mild (50 eV Ar^+) sputter cleaning. The solid red lines represent the linear extrapolation of the leading edge of the respective spectra. Note that "0"on the energy scale indicates the position of the Fermi edge E_F.

However, it is not clear whether the Cu-poor surface phase at the CIGSSe Back Surface is present from the beginning or whether its formation is induced by the lift-off process and subsequent exposure to N_2 atmosphere in the glovebox/glovebag or UHV, respectively.

In the past it was discussed whether the chalcopyrite/Mo interface results in an Ohmic contact [15-17] or whether a Schottky contact [18, 19] is formed. Kohara *et al.* even suspected the observed $MoSe_2$ layer to be responsible for an Ohmic contact at the chalcopyrite/Mo interface [16]. In a conventional CIGSSe-based solar cell device the charge carriers are generated in the low-gap, p-type chalcopyrite absorber and are separated in the electric field caused by the pn-junction formed by depositing the wide-gap, n-type window material onto the absorber. Thus, the photogenerated electrons (holes) have to travel to the front (back) contact to be able to contribute to the photocurrent. In consequence, the bandoffset of the valence band at the CIGSSe/Mo interface has to be known in order to judge the quality of the interface in terms of unhindered current transport. Hence, in order to shed more light on the electronic properties of the chalcopyrite/Mo interface, also the CIGSSe Mo-side was additionally characterized by UPS and IPES. The corresponding spectra of a freshly cleaved sample are shown in Fig. 9. Again the VBM and CBM are determined by linear extrapolation of the leading edges of the UPS and IPES spectrum, respectively. The resulting surface band gap of (1.30 ± 0.15) eV agrees surprisingly well with that of MoS_2 (1.20 – 1.35 eV [19]), which confirms the preferred formation of MoS_2 over that of $MoSe_2$ at the CIGSSe/Mo interface as discussed above.

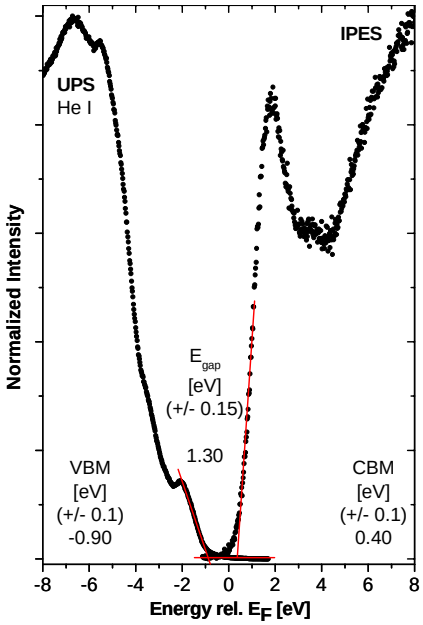

Fig. 9: UPS and IPES spectra (black dots) and VBM, CBM, and surface band gap values of a freshly cleaved CIGSSe Mo-Side sample. The solid red lines represent the linear approximation of the leading edge of the respective spectra. Note that "0" on the energy scale indicates the position of the Fermi edge E_F.

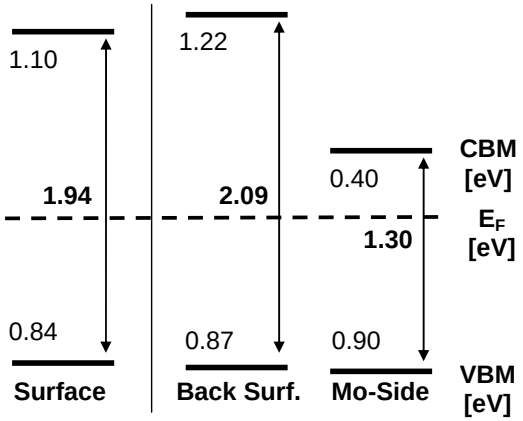

Fig. 10: Schematic summary of the valence band maxima (VBM), conduction band minima (CBM), electronic surface band gaps, and Fermi energy position. All numbers are given in eV and have an error of 0.10 eV (VBM and CBM) and 0.15 eV (band gaps).

The scheme in Fig. 10 shows a summary of the positions of the valence band maxima, the conduction band minima and the surface band gaps for all investigated samples. Neglecting any potential interface-induced band bending, Fig. 10 shows that the valence band at the CIGSSe/Mo(S_2) interface is (within the error bars) aligned and thus no barrier for hole transport across that interface is present. Furthermore, the conduction band at the CIGSSe Back is slightly higher than at the CIGSSe Surface, possibly suggesting the pres-

ence of a "back surface field" that repels minority charge carriers (electrons) from the CIGSSe/Mo interface.

2. The CdS/CIGSe interface

In Fall 2006, we received a set of CdS/CIGSe samples from NREL. For those samples the CdS layer thickness was varied by means of taking the samples out of the chemical deposition bath after different times (0 - 16 min). See Table II for a complete list. All samples were characterized by X-ray emission spectroscopy (XES) and XPS.

Fig. 11 shows the respective XES spectra of the Cd $M_{4,5}$ and In $M_{4,5}$ emission region on a linear (left) and logarithmic scale (right). Already after a deposition time of 1 min (and above), a Cd $M_{4,5}$ emission can be clearly identified (in particular on the logarithmic scale), which steadily increases with increasing deposition time. Consequently, the In $M_{4,5}$ emission intensity from the CIGSe substrate decreases due to the attenuation by the increasingly thick CdS layer. Close inspection of the data shows that the In $M_{4,5}$ emission is small, but still visible after a deposition time of 16 min. In order to quantify the thickness of the CdS layer using the XES data, we compared the CdS/CIGSe data with (reference) spectra of a thick CdS layer (not shown) and of the uncovered CIGSe substrate (bottom spectrum in Fig. 11). All measured spectra were described (in terms of a χ^2 fit) as a sum of the (weighted) reference CdS and substrate spectra:

$$\text{sample} = a \cdot \text{CdS}_{\text{reference}} + b \cdot \text{substrate} \quad (2)$$

To derive the thickness of the CBD-CdS layer deposited on CIGSe, we can use both, the attenuation of the In $M_{4,5}$ signal as well as the increase of the Cd $M_{4,5}$ intensity independently. If a homogeneous cover layer of thickness x attenuates the emission from the substrate, then the attenuated substrate emission intensity $I^{sub}(x)$ can be written as

$$I^{sub}(x) = I^{sub}_{ref} \cdot e^{-\frac{x}{\lambda^*}} \quad (3).$$

Similarly, the intensity of the emission from the cover layer $I^{cov}(x)$ can be written as

Table II

Sample	CdS Deposition Time
C2106-11	0 min, bare absorber
C2106-21	1 min
C2106-12	2 min
C2106-22	4 min
C2106-18	8 min
C2106-23	(2 × 8) 16 min

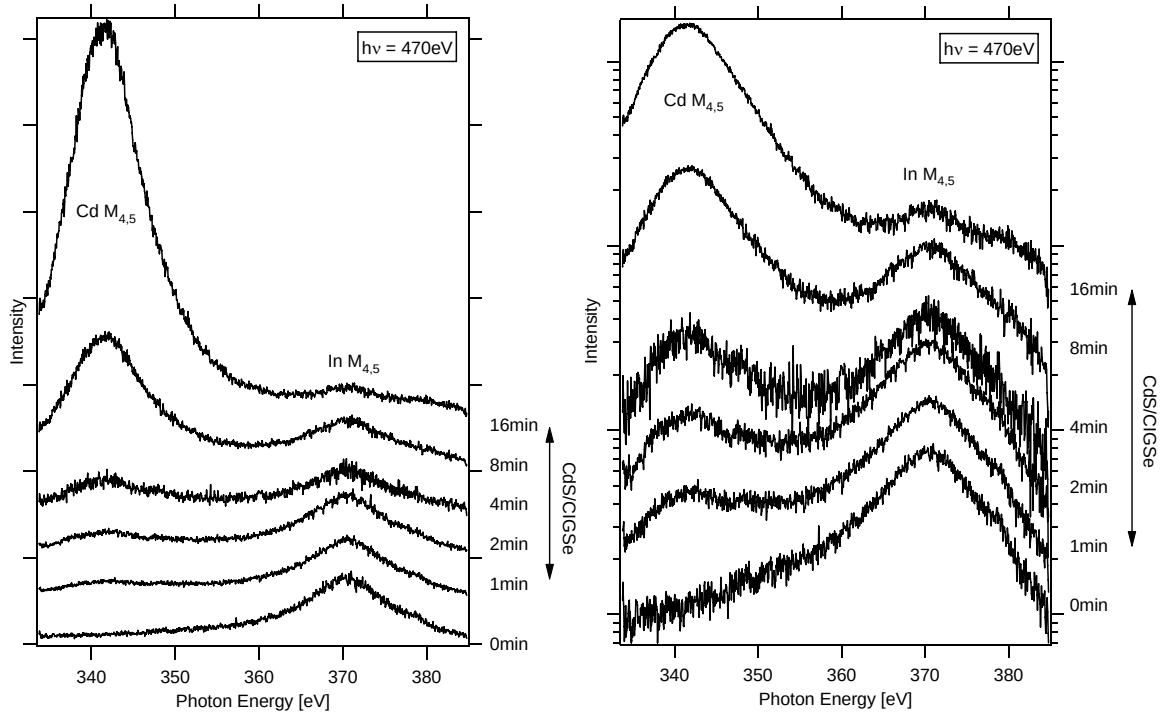

Fig. 11: Cd $M_{4,5}$ and In $M_{4,5}$ X-ray emission spectroscopy of the investigated set of CdS/CIGSe samples on a linear (left) and logarithmic scale (right).

$$I^{cov}(x) = I_{ref}^{cov}\left(1 - e^{-\frac{x}{\lambda^*}}\right) \quad (4)\,.$$

I_{ref}^{sub} and I_{ref}^{cov} denote the reference emission intensity of an uncovered substrate and of a cover layer of sufficient thickness, respectively ("sufficient" corresponds to a material thickness that results in a saturated emission intensity). Furthermore,

$$\frac{1}{\lambda^*} = \left(\frac{1}{\lambda_{exc}\cdot\sin\alpha}\right) + \left(\frac{1}{\lambda_{em}\cdot\sin\beta}\right) \quad (5),$$

where λ_{exc} and λ_{em} are the attenuation lengths in the cover layer for the excitation and

Table III
X-ray attenuation lengths in CdS (taken from [21]).

λ_{CdS} Cd $M_{4,5}$ emission (341.3 eV)	λ_{CdS} In $M_{4,5}$ emission (370.4 eV)	λ_{CdS} excitation (470.0 eV)
189 nm	216 nm	128 nm

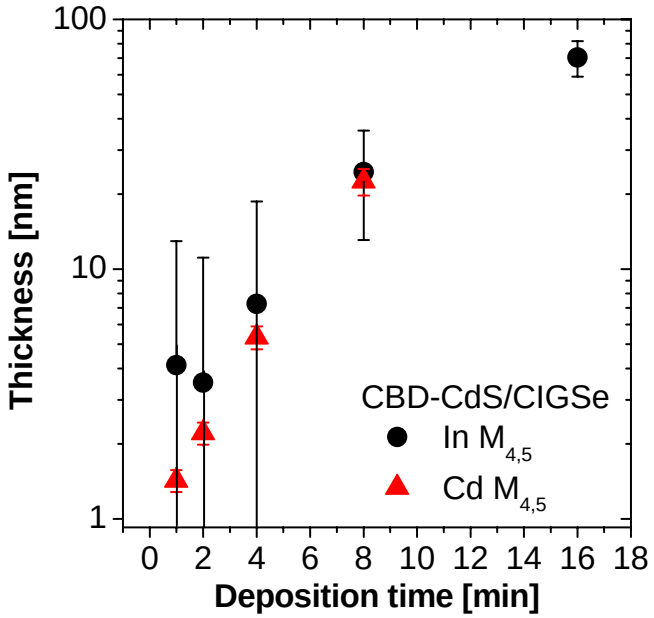

Fig. 12: CdS layer thickness determined from the attenuation of the In $M_{4,5}$ emission of the substrate or from the increase of the Cd $M_{4,5}$ emission from the cover layer, respectively.

emission energy, respectively. α and β are the angles of excitation and emission relative to the sample surface, respectively (in our case α = β= 45°). In order to obtain the cover layer thickness x, we used the above-determined weighting factors $a = I^{cov}(x) : I^{cov}_{ref}$ and $b = I^{sub}(x) : I^{sub}_{ref}$ (see Eq. 2). The attenuation lengths associated with the Cd $M_{4,5}$ and In $M_{4,5}$ emission energies, the excitation energy, and the specific overlayer material (here: CdS) are listed in Table III. Assuming that the CdS layer homogeneously covers the substrate (as it can be expected if prepared by a wet-chemical deposition method such as CBD), the layer thicknesses on CIGSe were determined and are shown in Fig. 12 as a function of the deposition time. The given error is assumed to be dominated by the uncertainty in comparing absolute XES intensities due to sample (mis)alignment and is estimated to be 10% for the above-mentioned intensity ratios. For deposition times of 2 min and above, the values determined using the attenuation of the In $M_{4,5}$ CIS emission are (within the error bars) quite similar to those calculated from the increasing Cd $M_{4,5}$ cover layer emission intensity. Thus, both approaches (Eq. (3) and (4)) give consistent numbers. For thin cover layers the thickness determination based on the Cd $M_{4,5}$ emission intensity is more reliable as indicated by the smaller error bars. The thickness of the CBD-CdS layer after a deposition time of 16 min (which corresponds to the standard CdS buffer) on CIGSe is determined to be (70 ± 11) nm.

S $L_{2,3}$ spectra of the investigated set of samples and of a CdS reference were also recorded. They are shown in Fig. 13, again on a linear (left) and a logarithmic scale (right). The main peak of the CdS reference spectrum at 147.3 eV (which is actually a doublet indicated by the clearly visible shoulder at 149 eV) is due to S 3s electrons de-

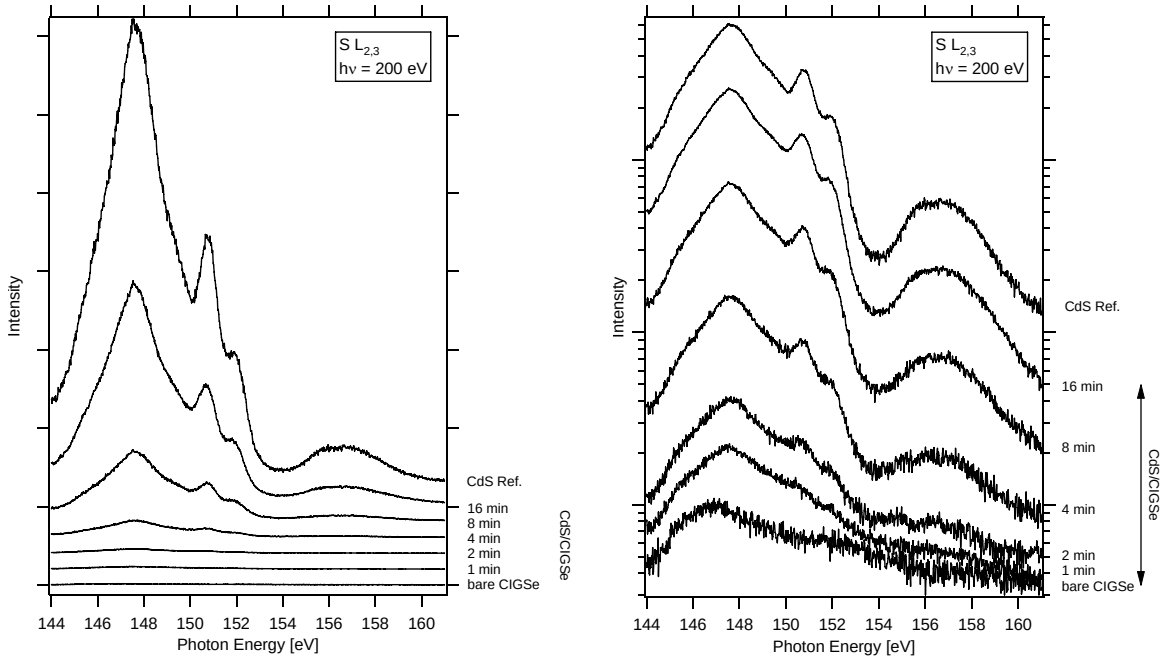

Fig. 13: S $L_{2,3}$ emission of the investigated set of CdS/CIGSe samples on a linear (left) and logarithmic scale (right). For comparison also the spectrum of a CdS reference is shown.

caying into S $2p_{1/2}$ and S $2p_{3/2}$ core holes. In addition, the two peaks at 150.5 eV and 151.8 eV correspond to Cd 4d electrons decaying into the S $2p_{1/2}$ and S $2p_{3/2}$ core holes, respectively. They thus directly indicate sulfur atoms bound to Cd. Furthermore, we observe the upper valence band of CdS at about 156 eV. Comparing the spectra of the CdS/CIGSe samples with that of the CdS reference, it is obvious that they also show the typical features of a CdS S $L_{2,3}$ spectrum, especially when compared on logarithmic scale. As expected, this gets more distinct with increasing deposition time.

In an earlier paper [22], the absence of the features indicating S-Cd bonds was indicative of intermixing processes at the CdS/CIGSe interface. For a detailed evaluation of whether such effects also play a role here, the new spectra are shown in Fig. 13, left, with a normalization to their maximum. It can be observed that the spectrum of the bare (S-free!) CIGSe substrate shows different spectral features compared to the spectra of the S-containing samples. A magnified (smoothed) presentation of the CIGSe XES spectrum shown in Fig. 14 (right) reveals two spectral features, which are separated by 5.7 eV. Since the latter agrees well with the doublet separation of Se $3p_{1/2}$ and Se $3p_{3/2}$, the features can most likely be attributed to Se 4s electrons decaying into Se $3p_{1/2}$ and Se $3p_{3/2}$ core holes. Note that our group has (for the last ten years) repeatedly searched for such Se 3p emission peaks; only recently, a significant improvement of the XES spectrometer has made it possible to observe such very weak structures.

A similar analysis approach as used above (i.e., describing the CdS/CIGSe spectra as a sum of the weighted reference CdS- and CIGSe-spectra) was used to clarify whether the intensity ratio between the features directly indicating S-Cd bonds and the main S 3s peak changes with deposition time or whether the spectra of the CdS/CIGSe samples can be

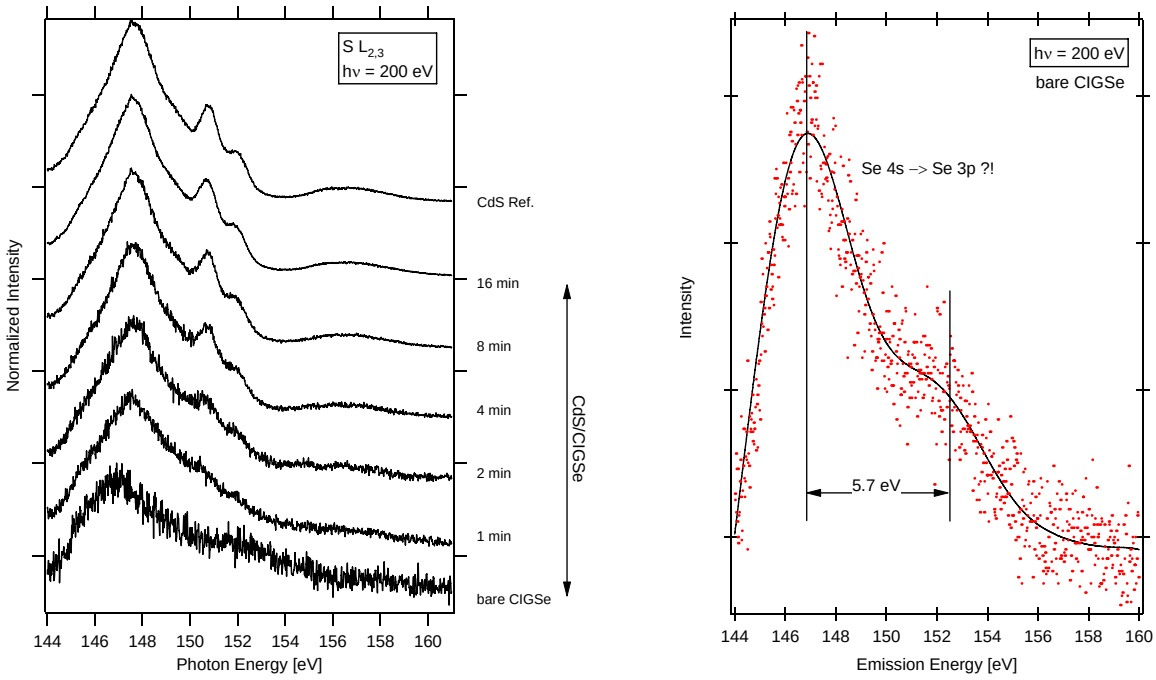

Fig. 14: Normalized S $L_{2,3}$ emission of the investigated set of CdS/CIGSe samples (left). Magnified and smoothed presentation of the spectrum of the bare CIGSe sample (right): red dots: original data, black solid line: smoothed spectrum.

explained by a (weighted) superposition of CdS and bare CIGSe reference spectra. The exemplary comparison of the experimental data of the "1 min" sample with a respective fit is shown in Fig. 15. The fit agrees quite well with the experimental data except between 150 -153 eV (the spectral range of the features directly indicating S-Cd bonds). We thus conclude that the spectra taken for thin CdS films can not be explained by a mere superposition of the Se substrate signal and the CdS reference. Nevertheless, in contrast to our earlier work, we find a clear Cd 4d signature (albeit smaller than for the CdS reference) even for the thinnest CdS film. Surface-sensitive XPS experiments in Fig. 16 additionally show that after 16 min deposition the Se 3d XPS signal vanishes, which is again in contrast to earlier experiments on CdS/CIGSe samples from a different source [22].

This can be interpreted in the following way: We do not find any evidence for a significant S/Se intermixing process. Nevertheless, the environment of the sulfur atoms at the growth start of the interface clearly deviates from a perfect CdS environment. Whether this is due to a less perfect crystalline structure (i.e., the formation of very small nm-scale nanoparticles [23]) or some sulfur diffusing into the CIGSe absorber can not unambiguously be differentiated.

Furthermore, the sample set was also characterized by UPS and IPES in order to determine the electronic interface structure. The evaluation of this data is still ongoing and will be presented in a future report.

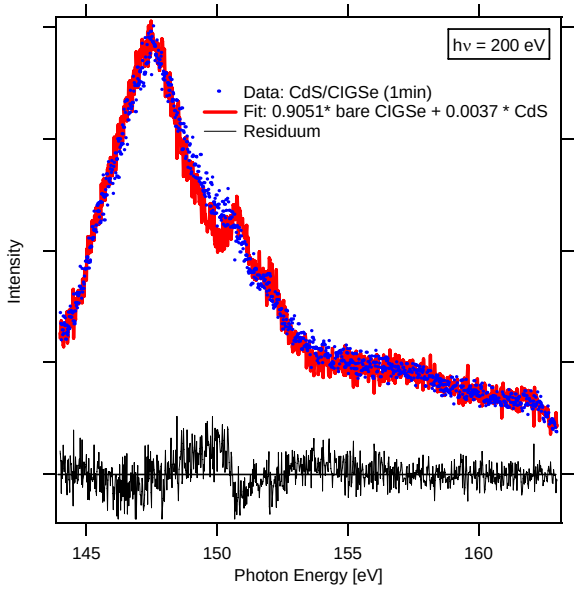

Fig. 15: Comparison of the 'S $L_{2,3}$ spectrum' of the "1 min" CdS/CIGSe sample with a weighted superposition fit. In addition, also the residuum (difference between data and fit) is shown.

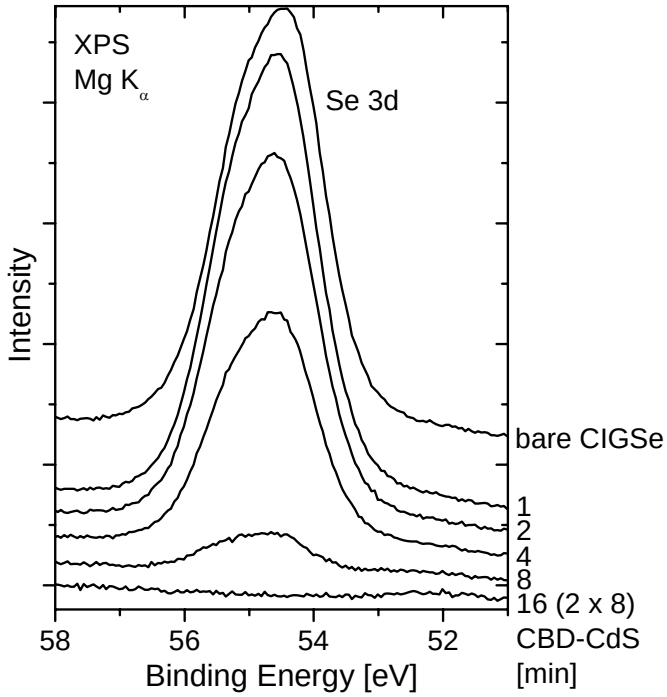

Fig. 16: Se 3d XPS detail spectra of the CdS/CIGSe sample set.

References:

[1] L. Weinhardt, O. Fuchs, A. Peter, E. Umbach, C. Heske, J. Reichardt, M. Bär, I. Lauermann, I. Kötschau, A. Grimm, S. Sokoll, T.P. Niesen, S. Visbeck, and F. Karg, J. Chem. Phys. **124**, 074705 (2006).
[2] L. Weinhardt, M. Blum, M. Bär, C. Heske, O. Fuchs, E. Umbach, J.D. Denlinger, K. Ramanathan, and R. Noufi, presented at the European Materials Research Society Spring Meeting, Nice, France, 29.5.-2.6.2006, Thin Solid Films **515**, 6119 (2007).
[3] Th. Glatzel, D. Fuertes Marron, Th. Schedel-Niedrig, S. Sadewasser, and M. Ch. Lux-Steiner, Appl. Phys. Lett. **81**, 2017 (2002).
[4] V. Probst, W. Stetter, W. Riedl et al., Thin Solid Films **387**, 262 (2001).
[5] N. Kohara, S. Nishiwaki, Y. Hashimoto, T. Negami, and T. Wada, Sol. Energy Mater. Sol. Cells **67**, 209 (2001).
[6] R. Scheer and H.-J. Lewerenz, J. Vac. Sci. Technol. A **13**, 1924 (1995).
[7] D. Schmid, J. Kessler, and H. W. Schock, Proceedings of the 12th European Photovoltaic Solar Energy Conference, Amsterdam, 653 (1994).
[8] J. H. Scofield, J. Electron Spectr. Rel. Phenomena **8**, 129 (1976).
[9] M. Bär, W. Bohne, J. Röhrich, E. Strub, S. Lindner, M.C. Lux-Steiner, Ch.-H. Fischer, T.P. Niesen, F. Karg, J. Appl. Phys. **96**, 3857 (2004).
[10] M. Morkel, L. Weinhardt, B. Lohmüller, C. Heske, E. Umbach, W. Riedl, S. Zweigart, and F. Karg, Appl. Phys. Lett. **79**, 4482 (2001).
[11] L. Weinhardt, M. Morkel, Th. Gleim, S. Zweigart, T.P. Niesen, F. Karg, C. Heske, and E. Umbach, Proc. 17th EuPVSC, Munich, Germany, p. 1261 (2001).
[12] L. Weinhardt, M. Bär, H. -J. Muffler, Ch. -H. Fischer, M. C. Lux-Steiner, T. P. Niesen, F. Karg, Th. Gleim, C. Heske, and E. Umbach, Thin Solid Films **431-432**, 272 (2003).
[13] D. Schmid et al., J. Appl. Phys. **73**, 2902 (1993).
[14] R. Schaffler et al., Diffusion and Defect Data B **51-52**, 347 (1996).
[15] A. J. Nelson, D. Niles, L. L. Kazmerski, D. Rioux, R. Patel, and H. Höchst, J. Appl. Phys. **72**, 976 (1992).
[16] N. Kohara, S. Nishiwaki, Y. Hashimoto, T. Negami, and T. Wada, Sol. Energy Mater. Sol. Cells **67**, 209 (2001).
[17] W. N. Shafarman and J. E. Phillips, Proceedings of the 25th IEEE Photovoltaic Specialists Conference, Washington, DC, 1996, p. 917.
[18] P. E. Russell, O. Jamjoum, R. K. Ahrenkiel, L. L. Kazmerski, R. A. Mickelsen, and W. S. Chen, Appl. Phys. Lett. **40**, 995 (1982).
[19] W. Jaegermann, T. Löher, and C. Pettenkofer, Cryst. Res. Technol. **31**, 273 (1996).
[20] J. Pouzet, H. Hadouda, J. C. Bernede, and R. Le Ny, J. Phys. Chem. Sol. **57**, 1363 (1996).
[21] B.L. Henke et al., *Atomic Data and Nuclear Data Tables* **54**, 181 (1993); http://www-cxro.lbl.gov/optical_constants/atten2.html.
[22] C. Heske, D. Eich, R. Fink, E. Umbach, T. van Buuren, C. Bostedt, L. J. Terminello, S. Kakar, M. M. Grush, T. A. Callcott, F. J. Himpsel, D. L. Ederer, R. C. C. Perera, W. Riedl, and F. Karg, Appl. Phys. Lett. **74**, 1451 (1999).
[23] Ch. Barglik-Chory et al., Chem. Phys. Lett. **379**, 443 (2003).

Project presentations (talks, unless marked as "Poster")

1. C. Heske, "Surface and interface analysis in Las Vegas", Seminar Experimentelle Physik II, University of Würzburg, Germany, July 20, 2006.
2. C. Heske, "Characterizing surfaces and interfaces in thin film solar cells by soft X-ray spectroscopy", Symposium: PHOTOVOLTAICS, SOLAR ENERGY MATERIALS and THIN FILMS, XV International Materials Research Congress, Cancun, Mexico, August 2006.
3. C. Heske, "How to reveal the chemical and electronic properties of interfaces, buried layers, and liquids with soft x-ray spectroscopy", Materials Science and Engineering Department, Stanford University, August 31, 2006.
4. C. Heske, "How to reveal the chemical and electronic properties of interfaces, buried layers, and liquids with soft x-ray spectroscopy", Physics Department, Boston University, December 8, 2006.
5. M. Bär, "Chemical and Electronic Properties of the Front and Back Surfaces of Chalcopyrite Thin Film Solar Cell Absorbers", 2007 MRS Spring Meeting, San Francisco, April 2007.
6. L. Weinhardt, "X-ray and electron spectroscopy investigation of interfaces and surfaces in CdTe thin film solar cells", 2007 MRS Spring Meeting, San Francisco, April 2007.
7. J. Zhou, "The mechanism of J-V "roll-over" in CdS/CdTe devices", 2007 MRS Spring Meeting, San Francisco, April 2007.
8. C. Heske, "Introduction" at the Young Scientist Tutorial, 2007 MRS Spring Meeting, San Francisco, April 2007.
9. M. Bär, L. Weinhardt, "Surface/interface characterization and modification" at the Young Scientist Tutorial, 2007 MRS Spring Meeting, San Francisco, April 2007.
10. C. Heske (Poster), "Characterization of the electronic and chemical structure at $Cu(In,Ga)(S,Se)_2$ and CdTe thin film solar cell interfaces", 2007 Solar Review Meeting, Denver, April 2007.
11. C. Heske, "Surface and Interface Analysis of Real-World $Cu(In,Ga)(S,Se)_2$ Thin Film Solar Cells", Global Solar, Tucson, AZ, July 2007.
12. M. Bär, "Bandoffset Tailoring – A Tool To Improve Thin Film Solar Cells", Hahn-Meitner-Institute, Berlin, July 2007.

Submitted articles (deliverable: one submitted journal article, one or more submitted conference article)

1. Journal: "Chemical properties of the Cu(In,Ga)Se_2/Mo/glass interfaces in thin film solar cells", L. Weinhardt, M. Blum, M. Bär, C. Heske, O. Fuchs, E. Umbach, J.D. Denlinger, K. Ramanathan, and R. Noufi, Thin Solid Films **515**, 6119-6122 (2007).
2. Journal: "Surface modifications of Cu(In,Ga)S_2 thin film solar cell absorbers by KCN and H_2O_2/H_2SO_4 treatments"**,**
   L. Weinhardt, O. Fuchs, D. Groß, E. Umbach, C. Heske, N.G. Dhere, A.A. Kadam, and S.S. Kulkarni, J. Appl. Phys. **100**, 024907 (2006).
3. Conference: "The mechanism of J-V "roll-over" in CdS/CdTe devices", J. Zhou, X. Wu, Y. Yan, S. Asher, J. L. F. Da Silva, Su-Huai Wei, L. Weinhardt, M. Bär, and C. Heske, Proc. 2007 MRS Spring Meeting, San Francisco, April 2007.
4. Conference: Characterization of the electronic and chemical structure at Cu(In,Ga)(S,Se)$_2$ and CdTe thin film solar cell interfaces, M. Bär, L. Weinhardt, M. Blum, S. Pookpanratana, and C. Heske, Proc. 2007 Solar Review Meeting, Denver.

If you have any questions, please do not hesitate to call me at (702) 895-2694.

Sincerely,

C. Heske
Associate Professor
Department of Chemistry
University of Nevada, Las Vegas

CC: C. Lopez